NASA Technical Paper 1235

Investigation of Light Scattering as a Technique for Detecting Discrete Soot Particles in a Luminous Flame

David R. Schryer

JULY 1978

NASA

NASA Technical Paper 1235

Investigation of Light Scattering as a Technique for Detecting Discrete Soot Particles in a Luminous Flame

David R. Schryer
Langley Research Center
Hampton, Virginia

NASA
National Aeronautics
and Space Administration

**Scientific and Technical
Information Office**

1978

NASA Technical Paper 1235

Investigation of Light Scattering as a Technique for Detecting Discrete Soot Particles in a Luminous Flame

David R. Schryer
Langley Research Center
Hampton, Virginia

National Aeronautics
and Space Administration

**Scientific and Technical
Information Office**

1978

SUMMARY

An investigation has been made of the practicability of using a classical light-scattering technique to detect discrete soot particles (diameter less than 50 nm) in premixed propane/air and propane/oxygen-helium flames. The technique involved comparison of angular scattering intensity patterns with theoretically determined Mie and Rayleigh patterns. The experimental apparatus employed in this investigation included a laser light source, a flat-flame burner, specially coated optics, a cooled photomultiplier detector, and a lock-in voltmeter readout. Large, agglomerated soot particles were successfully detected and sized. It was not possible, however, to detect small, discrete particles. The limiting factor appeared to be background scattering by the system's optics.

INTRODUCTION

The formation of soot within combustion systems such as flames, gas turbines, etc., can lead to potential combustor and environmental problems. From a combustor aspect, the presence of soot can cause excessive heat transfer and resultant material problems; from the environmental aspect, the production and emission of soot can result in unwanted levels of smoke and influence atmospheric chemistry. For example, carbon surfaces are known to be catalytic for the conversion of SO_2 to sulfate (ref. 1) and may well be of importance in many other atmospheric reactions which are now considered to occur predominately in the gas phase. One of the principal objectives of studies of soot formation has been to determine the processes by which soot particles are formed. In order to understand these processes better, there is a need to obtain accurate data on the concentration, size, and size distribution of soot particles within the combustion environment. Therefore, the development of in situ techniques for sizing soot particles is of prime importance.

Studies of the size and structure of soot particles in flames have generally involved one or the other of two classes of techniques. One class of techniques involves extracting samples of soot from the flame and then analyzing the extracted soot with electron microscopy (refs. 2 to 8). One disadvantage of such sampling-microscopy techniques is that while they generally yield consistent results - namely, the existence of relatively large (100 to 300 nm) chainlike agglomerates made up of smaller (10 to 50 nm) essentially spherical particles - the smaller particles are rarely seen in discrete, unagglomerated form; and the extent to which the observed agglomeration has occurred in the sampling process, rather than in the flame, is not known. Thus, the true structure of soot in a flame is not revealed unambiguously by such techniques. Furthermore, the introduction of a sampling probe into a flame inevitably perturbs the flame in some fashion.

The second class of techniques used to study soot in flames involves light scattering which perturbs neither the flame nor the structure of the soot contained therein. Consequently, several investigators (refs. 7 to 10) have attempted to study soot, in situ, by using various light-scattering techniques. Unfortunately, most light-scattering techniques suffer from a problem which, although different from the problems of sampling-microscopy techniques, also results in bias toward larger particles. This problem is that the intensity of light scattering decreases sharply with decreasing particle size. Thus, if particles of more than one size are present in a volume element, the scattering from the larger particles can effectively mask the scattering from smaller particles. This may occur even if the larger particles are far less abundant. Even if the particle sizes are stratified so that particles of different sizes are not present in the same volume element, the scattering from small particles is very weak and difficult to detect. The problem cannot be alleviated simply by increasing the intensity of the incident light and/or the sensitivity of the detector since such approaches also increase the level of background light or noise detected and do not improve the signal to noise ratio. In view of the foregoing problem, it should not be surprising that most investigators using light-scattering techniques have detected the larger agglomerates and failed to detect the smaller discrete particles. Thus, their results are quite similar to those of sampling-microscopy studies.

It should be noted that each of the approximately spherical particles referred to in this report as "small," "discrete," and "unagglomerated" is in fact, believed to be made of several even smaller particles clustered tightly together. Particle growth at all stages is believed to involve both clustering of existing particles and deposition of additional carbonaceous material. When the existing particles are very small, growth by carbonaceous deposition competes successfully with clustering; thus, interparticle boundaries within each cluster are obscured so that the resultant small clusters appear to be discrete particles. Growth by deposition does not compete successfully with further clustering for particles as large as 10 to 50 nm; consequently, the resultant 100- to 300-nm agglomerates are clearly not discrete (ref. 6).

The present study constituted an attempt to refine the light-scattering technique in order to detect small, discrete particles and to observe the onset of agglomeration by using a combination of advanced components not used by, or not available to, earlier investigators. Unfortunately, this attempt too was unsuccessful. This report documents the experimental apparatus and techniques employed, including the various modifications evolved, and discusses the reasons why none were successful.

SYMBOLS

d	particle diameter, nm
I	light intensity, W/m^2
l	distance from scattering particles to detector, m

M	total mass of scattering particles in volume element scanned, kg
m	complex refractive index of scattering particles
N	number of scattering particles in volume element scanned
x	size parameter, $\pi d/\lambda$
θ	scattering angle, deg
λ	wavelength of incident light, nm
ρ	density of scattering particles, kg/m^3
ϕ,ϕ'	Mie scattering functions

Subscripts:

$\perp$	perpendicular
$\parallel$	parallel

Superscripts:

o	incident
s	scattered

THEORY AND BACKGROUND

The angular distribution functions for monochromatic light of wavelength λ scattered by homogeneous spherical particles of diameter d and complex refractive index m were derived exactly by Mie in 1908. Reference 9 presents the Mie equations in the following convenient form, with the notation of the present paper being used:

$$I_{\perp}^{s}(\theta) = \frac{\lambda^2 x^6}{4\pi^2 \ell^2} \phi_{\perp}(x,m,\theta) I_{\perp}^{o} \tag{1}$$

and

$$I_{\parallel}^{s}(\theta) = \frac{\lambda^2 x^6}{4\pi^2 \ell^2} \phi_{\parallel}(x,m,\theta) I_{\parallel}^{o} \tag{2}$$

Since $x = \pi d/\lambda$, equations (1) and (2) may be rewritten as

$$I_{\perp}^{s}(\theta) = \frac{\pi^4 d^6}{4\lambda^4 \ell^2} \phi_{\perp}'(d,m,\theta) I_{\perp}^{o} \tag{3}$$

and

$$I_{\parallel}^{s}(\theta) = \frac{\pi^4 d^6}{4\lambda^4 \ell^2} \phi_{\parallel}'(d,m,\theta) I_{\parallel}^{o} \tag{4}$$

These terms $\phi_{\perp}$, $\phi_{\parallel}$, $\phi_{\perp}'$, and $\phi_{\parallel}'$ are rather cumbersome functions involving Legendre polynomials and spherical Bessel functions and need not be written out here. Reference 11 presents complete statements of the Mie equations as well as details of their derivation.

The Mie equations only apply strictly to scattering by a single, homogeneous spherical particle. However, the scattering functions for a small volume element containing N such particles are simply N times the single-particle function, providing the particle density is sufficiently low so that the particles act independently (criterion of independent scattering) and the light is not scattered more than once (criterion of single scattering). (See ref. 11.) The criterion of independent scattering is considered to be met, in practice, when the mean separation of the scattering particles is at least three times the particle diameter. The practical criterion for single scattering is that the total extinction of the incident light be 10 percent or less. When these criteria are met, the Mie equations can be multiplied by N to yield the appropriate multiparticle scattering equations

$$I_{\perp}^{s}(\theta) = \frac{N\pi^4 d^6}{4\lambda^4 \ell^2} \phi_{\perp}'(d,m,\theta) I_{\perp}^{o} \tag{5}$$

and

$$I_{\parallel}^{s}(\theta) = \frac{N\pi^4 d^6}{4\lambda^4 \ell^2} \phi_{\parallel}'(d,m,\theta) I_{\parallel}^{o} \tag{6}$$

For particles that are small compared to the wavelength of the incident light, the Mie equations reduce to the much simpler Rayleigh equations (ref. 11) as follows:

$$I_{\perp}^{s}(\theta) = \frac{N\pi^4 d^6}{4\lambda^4 l^2}\left|\frac{m^2 - 1}{m^2 + 2}\right|^2 I_{\perp}^{o} \tag{7}$$

and

$$I_{\parallel}^{s}(\theta) = \frac{N\pi^4 d^6}{4\lambda^4 l^2}\left|\frac{m^2 - 1}{m^2 + 2}\right|^2 \cos^2\theta\, I_{\parallel}^{o} \tag{8}$$

The Rayleigh equations are excellent approximations of the much more complex Mie equations for particles which have circumferences that are a few tenths, or less, of a wavelength. In fact, the scattering from such particles is frequently referred to as "Rayleigh scattering"; the term "Mie scattering," although theoretically applicable to homogeneous spherical particles of any size, is frequently applied only to particles too large for the Rayleigh approximation but too small for physical optics.

It is instructive to express the angular scattering functions in terms of the total mass rather than in terms of the number of scattering particles in a particular volume element. If the particles are assumed to be spherical with density ρ, their total mass M would be $\pi N\rho d^3/6$; therefore,

$$I_{\perp}^{s}(\theta) = \frac{3M\pi^3 d^3}{2\rho\lambda^4 l^2}\,\phi_{\perp}'(d,m,\theta)\, I_{\perp}^{o} \tag{9}$$

and

$$I_{\parallel}^{s}(\theta) = \frac{3M\pi^3 d^3}{2\rho\lambda^4 l^2}\,\phi_{\parallel}'(d,m,\theta)\, I_{\parallel}^{o} \tag{10}$$

If the variation of $\phi_{\perp}'$ and $\phi_{\parallel}'$ with d is neglected, it can be seen that $I^s \propto d^3$. Thus, a given mass of soot in the form of 250-nm agglomerates, for example, would scatter light 1000 times more intensely than would the same mass of soot in the form of 25-nm discrete particles.

As noted in the Introduction, soot is believed to be made up of small, roughly spherical particles (10 to 50 nm), many if not most of which agglomerate into larger chainlike clusters (100 to 300 nm). The ranges 10 to 50 nm and 100 to 300 nm correspond to Rayleigh scattering and Mie scattering, respectively, for visible light. Since very little soot is believed to be in the intermediate size range (50 to 100 nm), the distinction between discrete particles and agglomerates should be quite clear. The onset of agglomeration should be marked by an abrupt transition from Rayleigh to Mie scattering and a correspondingly sharp increase in scattering intensity, provided that the various particle sizes are stratified by such a technique as the use of a flat flame.

Several techniques for sizing particles by using light-scattering data have been proposed (refs. 7, 9, and 10). The most straightforward technique involves calculating theoretical scattering patterns for a range of particle sizes and comparing them with experimentally observed patterns. Particle size is then taken to be that of the theoretically calculated pattern that best fits the experimental data. At least three factors, however, complicate this technique:

(1) More than one size particle may be present in the volume element studied. Presumably this can be obviated, as just noted, by stratifying the sizes. If this is not accomplished, the largest particles present in any significant quantity will generally predominate.

(2) Particles are rarely spherical as assumed in the Mie theory and its limiting case, the Rayleigh theory. It is convenient to accept the fact that the theoretical and experimental scattering patterns for nonspherical particles will not fit exactly but to assume that the best fit indicates the size of "equivalent" spherical particles having similar scattering characteristics. Thus, the diameter "measured" for most real particles represents an approximation.

(3) Calculation of the theoretical scattering patterns depends on the complex refractive index of the particles under consideration. The refractive index of soot varies with its composition and temperature and is rarely, if ever, known exactly for conditions in a flame. Sometimes a refractive index for a compacted, room-temperature sample of soot from the flame being studied is used, and sometimes a theoretical value is calculated for ideal graphitic particles at the flame temperature. Since real soot is not pure carbon and is not perfectly graphitized, theoretically calculated values of the refractive index are as defective as the alternative values measured at room temperature. The uncertainty of the refractive index of soot under flame conditions is, by itself, sufficient to cast considerable doubt on any results obtained by a light-scattering technique. However, it should not prevent distinction between discrete and agglomerated particles, nor detection of the transition from one to the other.

It should be noted that if small, discrete particles could be detected by observing Rayleigh scattering patterns, the particles could not be sized because - apart from the problem of uncertainties in the refractive index - there is the additional problem in the Rayleigh size range that the shape of

the scattering patterns is independent of particle size. The absolute intensity of scattering at a given angle varies with size in the Rayleigh range; but, because the intensity also varies with particle concentration, it is impossible to distinguish between the two effects from scattering data alone. Nevertheless, if Rayleigh scattering attributable to soot is detected, it does place an approximate upper limit on the size of the particles. Furthermore, if the shape of the scattering patterns higher in the flame changed from Rayleigh to Mie with a sharp increase in intensity, the onset of agglomeration could reasonably be assumed. The observation of such a phenomenon was a primary goal of this study.

EXPERIMENTAL APPARATUS

The apparatus employed in this investigation is shown schematically in figure 1. Figure 2 is a photograph of the luminous flame laboratory at the Langley Research Center.

The burner used in all tests was a premixed flat-flame burner consisting of a cylindrical brass tube, 73-mm inside diameter, with inlet ports at the bottom for the fuel and oxidizer gases and a specially fabricated diffuser top through which the gases emerge well mixed with uniform flow velocity across the burner face. The diffuser top was fabricated from copper shot, which were hand sieved for uniform size by being passed through a 7-gage sieve and retained by an 8-gage sieve. The shot were tested for sphericity by rolling them down a shallow (about 15° slope) inclined plane; shot which did not reach the bottom on two consecutive tests were rejected. The resultant uniform size, essentially spherical, copper shot were fabricated into a monolithic cylindrical disk, 73 mm in diameter and approximately 35 mm thick, by pouring them into a graphite mold and sintering them in a vacuum furnace. A commercially available, fine-porosity sintered bronze faceplate 2 mm thick was then vacuum sintered to the surface of the resultant sintered copper disk, and this diffuser assembly was shrunk-fit into the top of the burner. The completed burner is shown in figure 3.

The excellent thermal and flow properties of the burner top contributed substantially to the attainment of a stable flat flame. Further control of flame stability was achieved by mounting a circular wire-mesh flame stabilizer above the burner. This flame stabilizer could be raised or lowered with an electric motor to achieve the optimum flame at various flow rates and fuel to oxidizer ratios. Figure 4 is a photograph of a typical flame. The burner was mounted in a chamber to obviate the problem of room drafts, and the chamber was evacuable to enable expansion of the flame reaction zone.

Propane was the fuel used in all tests of this study. Air was the oxidizing gas used initially, but a helium-oxygen analog of air was substituted when it was determined that scattering by the nitrogen molecules of air was significant. Helium has a significantly lower scattering efficiency than nitrogen.

The water contained in the combustion product gas tended to condense near the bottom of the chamber where the massive chamber baseplate was rela-

tively cool. The resultant cloud of water droplets produced very high levels of extraneous scattering. This problem was cured by heating the chamber bottom and by introducing a continuous flow of diluent gas into the chamber to decrease the partial pressure of water for a given total test pressure. Nitrogen was the diluent gas used initially, but helium was eventually substituted to reduce background scattering.

The light source used initially was a 5-mW helium-neon laser with a wavelength of 632.8 nm. Later this laser was replaced with a tunable argon ion laser whose strongest line was 514.5 nm with a maximum power of 3.2 W. The 514.5-nm line was used in all work involving this laser.

The detector used with the helium-neon laser was a 2-inch end window photomultiplier tube with an S-20 trialkali cathode. It was operated uncooled. The detector used with the argon ion laser was a 2-inch end window photomultiplier tube with an S-11 cesium antimony cathode which is more sensitive to 514.5-nm light than the S-20 cathode. The tube used was specified at purchase to be selected for highest quantum efficiency consistent with low dark current, a combination which yields a high signal to noise ratio. In order to further reduce the dark current, the tube was cooled to -40° C during operation.

The function of the detection system was to measure the relative intensity of that fraction of the incident light scattered at a given angle by the soot particles in the flame being investigated. In order to achieve this goal, it was essential to reject light from all other sources. Two devices were used to accomplish this rejection: (1) A narrow band-pass filter centered at the wavelength of the laser being used was interposed between the flame and the photomultiplier tube. (The rejection ratio of the filters used was 5000 to 1.) (2) To reject that fraction of ambient light, including light emitted by the luminous flame, which fell within the filter band pass, the incident laser light was chopped at a frequency of 260 Hz and the output of the photomultiplier tube was read out with a lock-in voltmeter which was synchronized with the chopper. The lock-in voltmeter thus read out only that component of the photomultiplier output pulsed with the same frequency and phase as the chopper. The lock-in voltmeter was capable of distinguishing and measuring the pulsed signal, even in cases where the background output of the photomultiplier from all sources was as great as, or slightly greater than, the properly pulsed signal.

In order to control the intensity of light which struck the photomultiplier tube, a stack of five neutral density filters of known transmissivity was employed. The individual filters, in any combination, could then be inserted into or withdrawn from the optical path between the flame and photomultiplier as needed.

The photomultiplier and associated optics were mounted on a rotatable base so that light scattered at various angles could be measured. In order to minimize variations in the intensity of the incident light, it was necessary for the laser beam to enter the chamber through a single optical port. To achieve the foregoing and to allow the photomultiplier to be rotated in a horizontal plane, it was necessary to have the laser beam enter the chamber vertically although the beam then traversed the flame horizontally. The small

helium-neon laser could be attached vertically to the chamber assembly, but the much larger argon ion laser had to rest horizontally on the floor. For convenience, the photomultiplier and its associated optics were mounted vertically. Thus, optical reflectors had to be employed - two with the helium-neon laser as the light source and three with the argon ion laser. Front-silvered mirrors were used at first, but they were found to scatter too much light; also, their reflective surfaces were literally destroyed by the more powerful argon ion laser. Consequently, dielectric reflectors with high-quality refractory coatings were eventually employed. The coatings were specified to have maximum reflectance for the wavelength and angle of incidence employed. Similarly, the optical ports into and out of the chamber were changed, first from plate glass to optical glass, then to optical glass coated for minimum reflectance with the wavelength employed and normal incidence.

A major problem involved in minimizing the background scattering intensity is disposition of the incident laser beam after it has traversed the flame. Because of the criterion for single scattering, the intensity of this beam after leaving the flame was always 90 percent, or more, of its initial value. With the helium-neon laser, it was possible to construct a baffle-type light trap which effectively dissipated this beam; but with the much more powerful argon ion laser, none of the various light-trap designs was effective. The most effective technique simply involved reflecting the exiting beam out of the chamber via an additional optical reflector and exit port.

Unfortunately, even the best optical coatings available scatter about 0.1 percent of the light incident upon them. Since this light was chopped laser light of the proper wavelength to pass through the narrow band-pass filter and the right pulse frequency and phase to be detected by the lock-in voltmeter, such extraneous scattered light was very troublesome - much more so than ambient room light or light from the flame itself, both of which were effectively blocked from detection. Ultimately it was the inability to adequately reduce the extraneous laser light which placed a limit on the experiment. Light scattered by soot in the flame could not be measured if the extraneous light was of equal or greater intensity. As a help in rejecting extraneous laser light, a lens and pinhole aperture were inserted between the flame and the photomultiplier detector. The volume element of the flame being studied was imaged on the aperture by the lens. This reduced the extraneous light problem but did not eliminate it. Once again, it should be noted that in attempting to detect particles in the Rayleigh size range even very low levels of extraneous light may exceed the scattering intensity from the particles themselves.

EXPERIMENTAL PROCEDURE

The experimental procedure employed was as follows: The system's optics were first checked and alined so as to (1) send the incident light beam horizontally across the center of the burner at a predetermined height, (2) focus the detector aperture on the incident beam at the center of the burner, and (3) reflect the exiting laser beam out of the chamber. These steps were accomplished with a minimum of scattering from the optics themselves.

Following the foregoing optical alinement, the burner was lit and the flame allowed to stabilize. Then the gas flow rates were adjusted to give a stable flame at the desired equivalence ratio. The stabilizing screen height was adjusted to provide optimum flame geometry, as evidenced by vertical sides and flat top and bottom. The chamber pressure was adjusted to the desired value, and a suitable diluent gas flow was implemented. Scattering intensity measurements were then made at various angles. At each angle, two measurements were made, one with a fuel-rich luminous flame and a second with a lean, nonluminous flame. The fuel and oxidizer flow rates corresponding to each condition were carefully measured and reproduced for each angle, and the flame was allowed to stabilize after each transition before scattering measurements were made.

The scattering intensities measured with the lean, nonluminous flame were assumed to be ambient values, or noise levels, and were subtracted from the intensities measured at the same angles with a rich, luminous flame. The resultant differences were taken as the true intensities of light scattered by the soot particles in the flame. Because the volume of the sample element observed varies angularly by $1/\sin\theta$, the intensity measurements were multiplied by $\sin\theta$ to cancel out this effect. It should be noted that references 7 and 8 erroneously give this multiplicative correction factor as $1/\sin\theta$.

Flames of various total flow rates, pressures, and equivalence ratios (the equivalence ratio is the actual fuel-air ratio divided by the stoichiometric fuel-air ratio) were studied at various heights above the burner top.

RESULTS

Scattering in excess of the background level was frequently detected. The angular variation of such scattering in any instance did not correspond to the characteristics of small spherical particles. Figure 5 presents two sets of scattering data for light polarized perpendicular to the plane of observation, chamber pressure of 600 torr (1 torr = 133.322 Pa), and equivalence ratios of 2.7 and 1.9. Also plotted are the theoretical Mie scattering patterns that best fit the data. These patterns correspond to particle sizes of 470 nm and 575 nm. The differences between the theoretical and experimental patterns are rather large and are believed to be due, in part, to the asphericity characteristic of large soot particles and, in part, to error in the value of the index of refraction. The value of the refractive index used in this study was $1.57 - 0.565i$, which was measured by Dalzell (ref. 12) using room temperature soot from a premixed propane/air flame.

Even allowing for the foregoing sources of error, the particles observed are apparently quite large - significantly larger than are normally observed in propane/air flames. However, it must be remembered that these data were obtained with propane/helium-oxygen flames which are different from propane/air flames because of the thermal and transport property differences between helium and nitrogen, the major constituents of the flame gases of the two types of flames.

Since this study was not intended to duplicate previous light-scattering studies in which larger particles were detected and measured, relatively little effort was devoted to the accumulation of large-particle scattering patterns. Rather, when large particles were observed, the experimental conditions were changed so as to favor smaller particles by decreasing the equivalence ratio while surveying the flame at the same height above the burner or by maintaining the equivalence ratio constant but surveying slightly lower in the flame. Such changes in experimental conditions invariably resulted in a sharp decrease in signal intensity to a level indistinguishable from the background intensity. In no case was it possible to observe the Rayleigh scattering patterns which should have been associated with small, discrete particles.

Since a sharp decrease in signal intensity accompanied every change in conditions intended to decrease particle size, it seems reasonable to assume that the desired particle size decrease had, in fact, been achieved but that the scattering intensity of the smaller, presumably unagglomerated, particles was less than the achievable background level. It is interesting to note that Roth and Gebhart (ref. 13) in their analysis of the practical lower limit of particle size measurable with a similar light-scattering technique arrived at a value of 50 nm. This value also happens to be the upper limit of the diameter of discrete particles believed to be present in most soots; therefore, the analysis of Roth and Gebhart, combined with the results of the present study, would seem to indicate that particles smaller than 50 nm cannot be detected by the classical scattering technique with apparatus presently available.

CONCLUDING REMARKS

The limited results obtained in this study regarding large soot particles generated in premixed propane/helium-oxygen flames seem to indicate that such particles are highly aspherical and significantly larger than their counterparts in propane/air flames. In both types of flame, the large particles are, in all probability, agglomerates of many smaller particles. The larger such agglomerates are, the less spherical they tend to be. This is consistent with the results of the study.

The failure of the present study to detect small, discrete particles of 50 nm or less, despite systematic attempts to do so, is believed to indicate that such particles cannot be detected by means of the classical scattering technique with apparatus presently available.

Langley Research Center
National Aeronautics and Space Administration
Hampton, VA 23665
May 23, 1978

REFERENCES

1. Novakov, T.; Chang, S. G.; and Harker, A. B.: Sulfates as Pollution Particulates: Catalytic Formation on Carbon (Soot) Particles. Science, vol. 186, no. 4160, Oct. 18, 1974, pp. 259-261.

2. Millikan, Roger C.: Non-Equilibrium Soot Formation in Premixed Flames. J. Phys. Chem., vol. 66, no. 5, May 1962, pp. 794-799.

3. Bonne, U.; Homann, K. H.; and Wagner, H. Gg.: Carbon Formation in Premixed Flames. Tenth Symposium (International) on Combustion, Combustion Inst., 1965, pp. 503-512.

4. Mayo, P. J.; and Weinberg, F. J.: On the Size, Charge, and Number-Rate of Formation of Carbon Particles in Flames Subjected to Electric Fields. Proc. R. Soc. London ser. A, vol. 319, no. 1538, Oct. 27, 1970, pp. 351-371.

5. Maraval, L.: Characteristics of Soot Collected in Industrial Diffusion Flames. Combust. Sci. & Technol., vol. 5, no. 5, July 1972, pp. 207-212.

6. Wersborg, B. L.; Howard, J. B.; and Williams, G. C.: Physical Mechanisms in Carbon Formation in Flames. Fourteenth Symposium (International) on Combustion, Combustion Inst., 1973, pp. 929-940.

7. Erickson, W. D.; Williams, G. C.; and Hottel, H. C.: Light Scattering Measurements on Soot in a Benzene-Air Flame. Combust. & Flame, vol. 8, no. 2, June 1964, pp. 127-132.

8. Dalzell, W. H.; Williams, G. C.; and Hottel, H. C.: A Light-Scattering Method for Soot Concentration Measurements. Combust. & Flame, vol. 14, no. 2, Apr. 1970, pp. 161-170.

9. Kunugi, M.; and Jinno, H.: Determination of Size and Concentration of Soot Particles in Diffusion Flames by a Light-Scattering Technique. Eleventh Symposium (International) on Combustion, Combustion Inst., 1967, pp. 257-266.

10. D'Alessio, A.; DiLorenzo, A.; Beretta, F.; and Venitozzi, C.: Optical and Chemical Investigations on Fuel-Rich Methane-Oxygen Premixed Flames at Atmospheric Pressure. Fourteenth Symposium (International) on Combustion, Combustion Inst., 1973, pp. 941-953.

11. Van de Hulst, H. C.: Light Scattering by Small Particles. John Wiley & Sons, Inc., c.1957.

12. Dalzell, William H.: Measurement of Soot Concentration in Flames. Sc. D. Thesis, Massachusetts Inst. Technol., 1965.

13. Roth, C.; and Gebhart, J.: Comments to the Lower Detection of a Laser Aerosol Spectrometer. Aerosole in Physik, Medizin und Technik, Ges. Aerosol. Forsch. e.V., 1973, pp. 36-40.

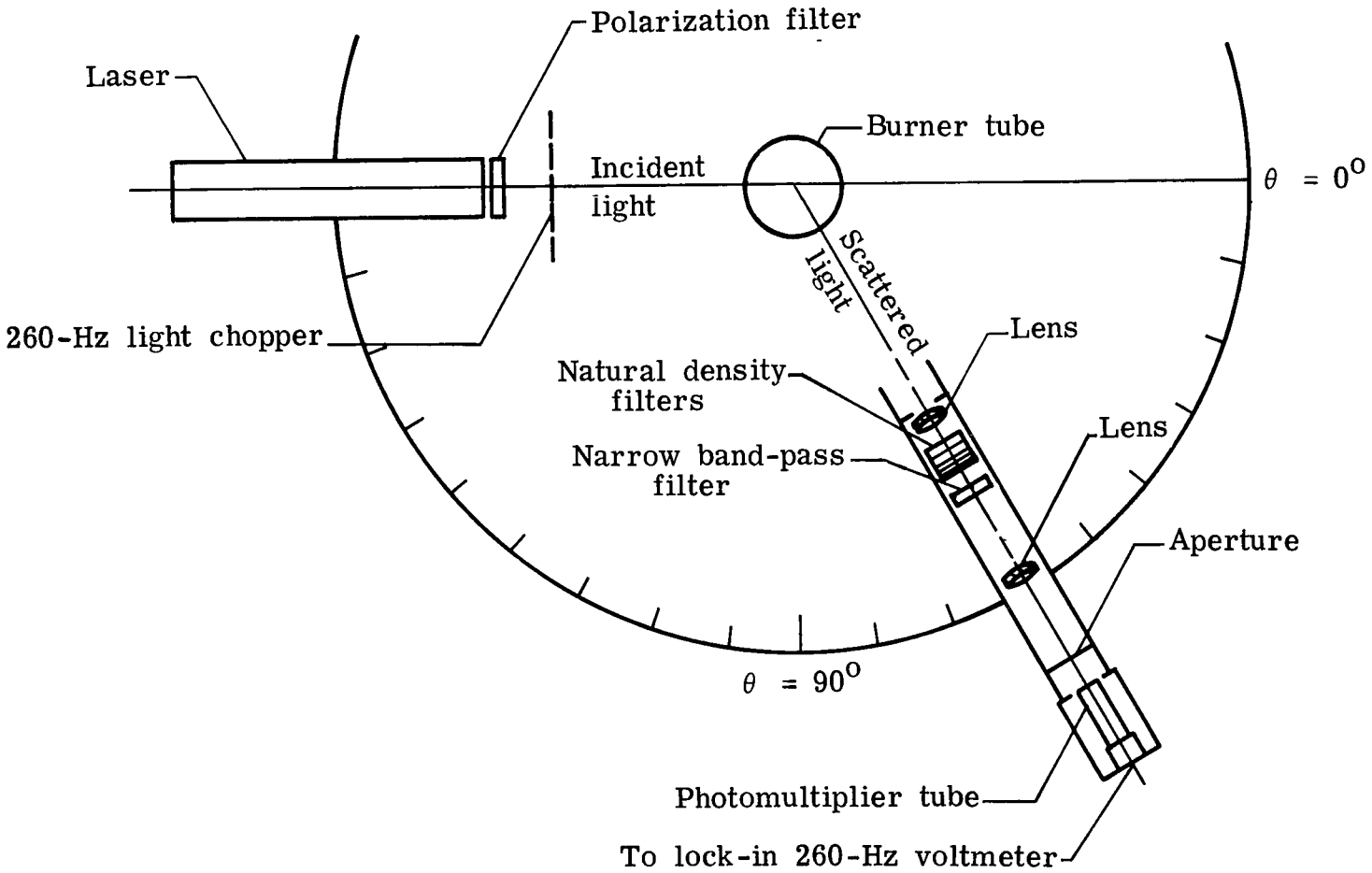

Figure 1.- Schematic of light-scattering apparatus.

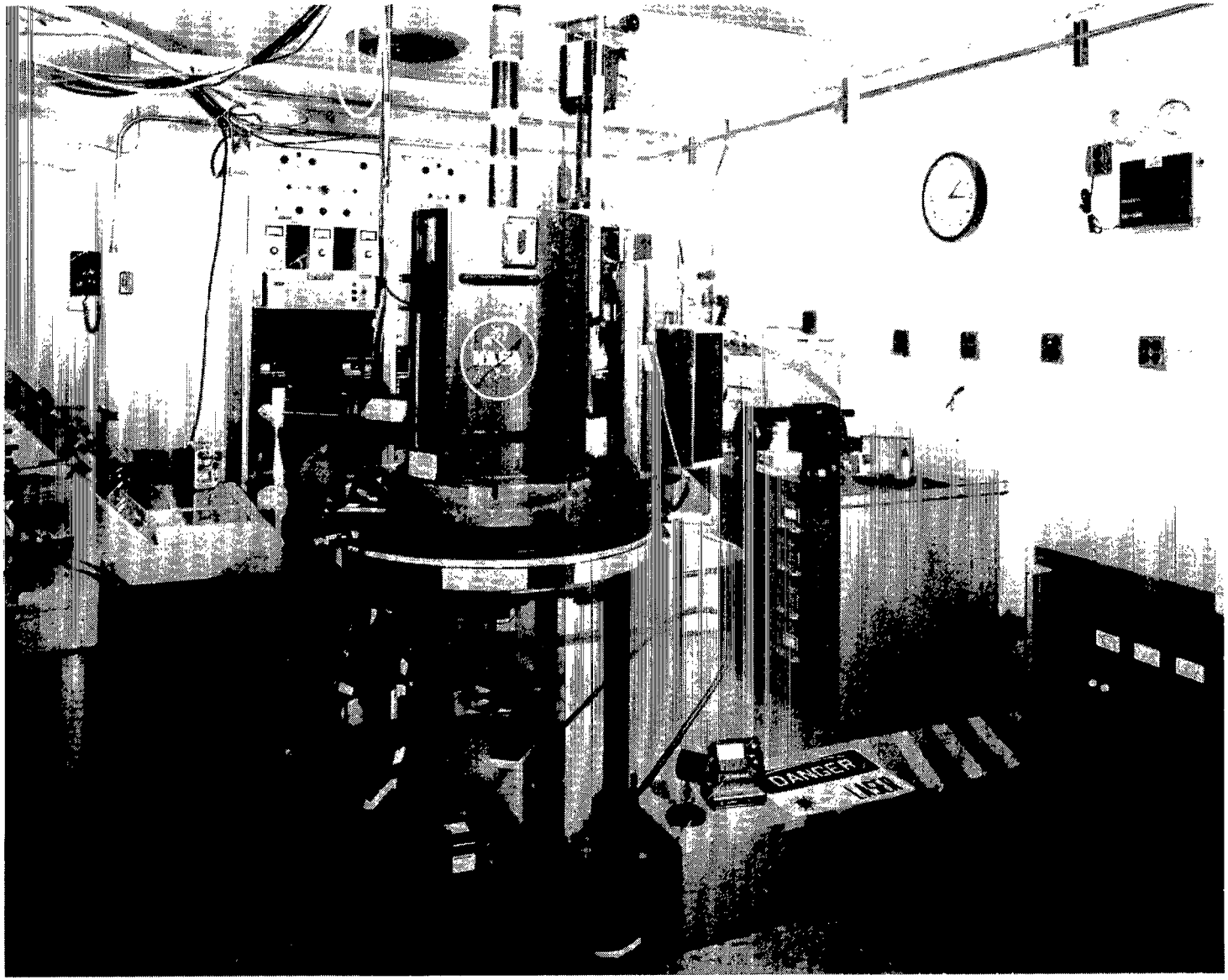

L-75-8840

Figure 2.- Luminous flame laboratory at the Langley Research Center.

L-74-1915

Figure 3.- Flat-flame burner.

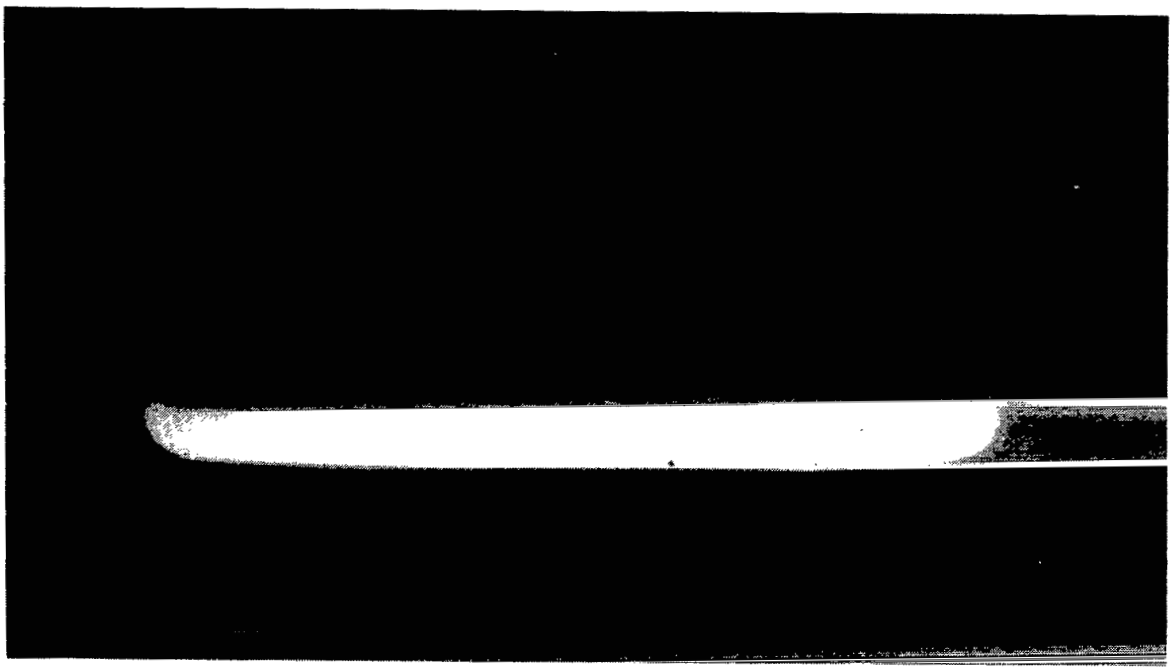

L-78-107

Figure 4.- Premixed propane/air flat flame.
Chamber pressure of 500 torr.

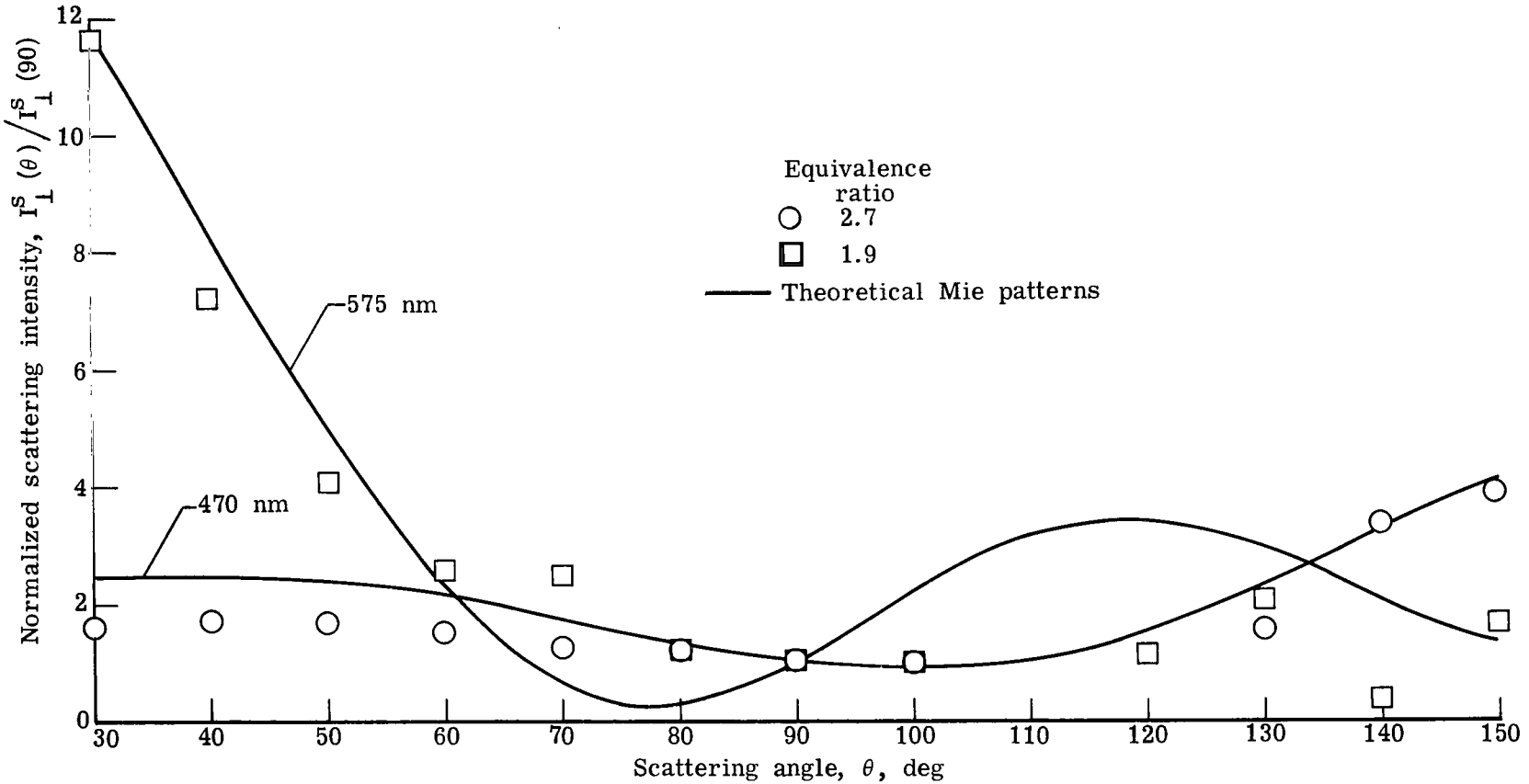

Figure 5.- Variation of normalized scattering intensity with scattering angle. Perpendicular polarization; chamber pressure of 600 torr; propane/helium-oxygen flat flame.

5 1 1U,H, 062378 S00903DS
DEPT OF THE AIR FORCE
AF WEAPONS LABORATORY
ATTN: TECHNICAL LIBRARY (SUL)
KIRTLAND AFB NM 87117